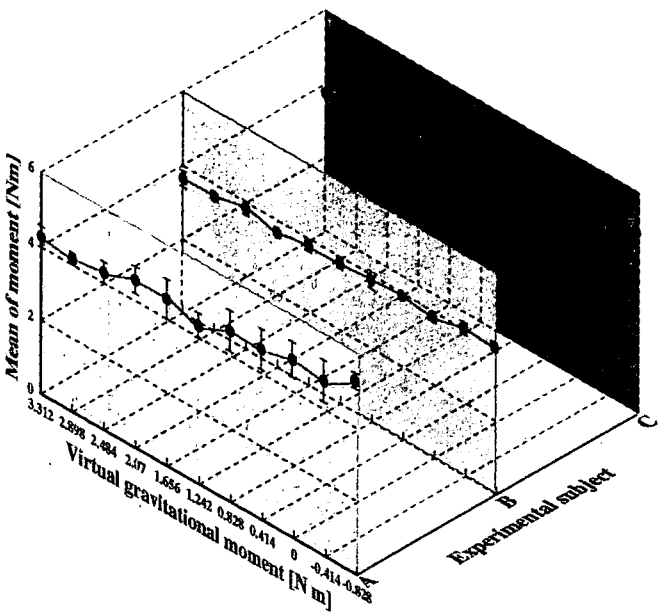

(c)

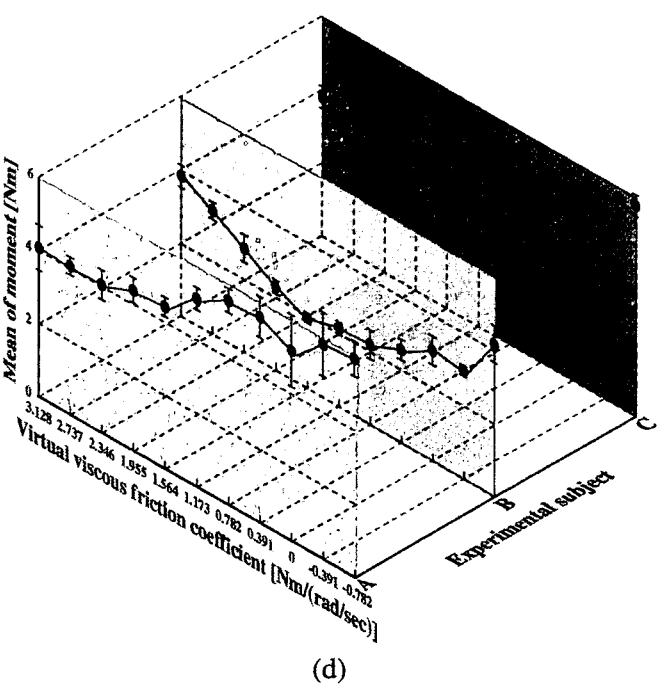

(d)

Figure 6. (Continued).

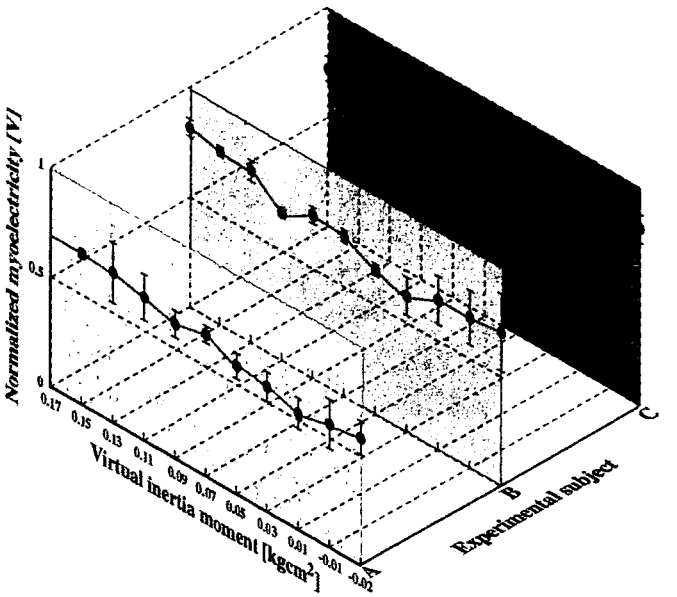

(a)

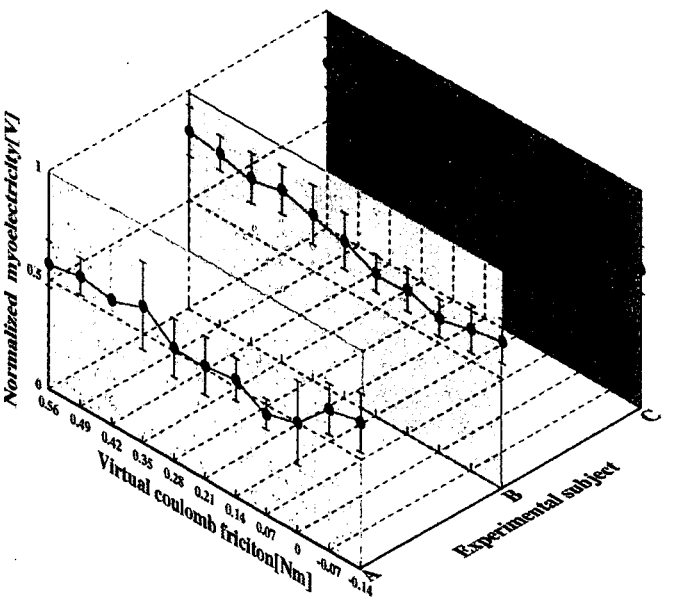

(b)

Figure 7. Experimental results for myoelectricity at the flexor muscle.

increased suddenly after they kept steady or increased slightly. Thus, what the results make clear is that the ideal virtual viscous friction for unconstrained motion was not zero. It is considered as the main cause of the results that the inertia

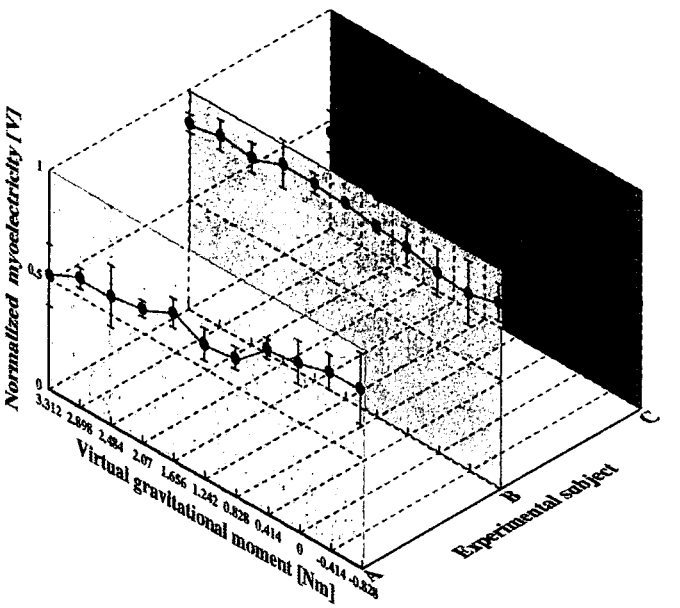

(c)

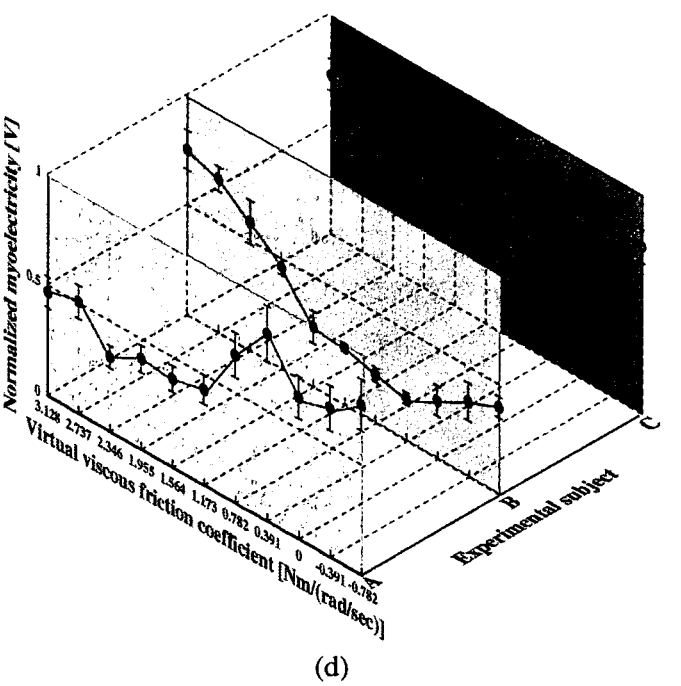

(d)

Figure 7. (Continued).

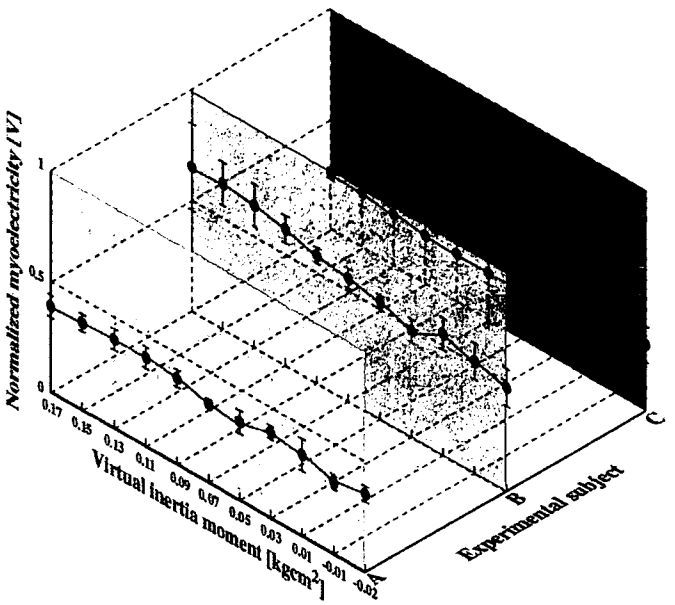

(a)

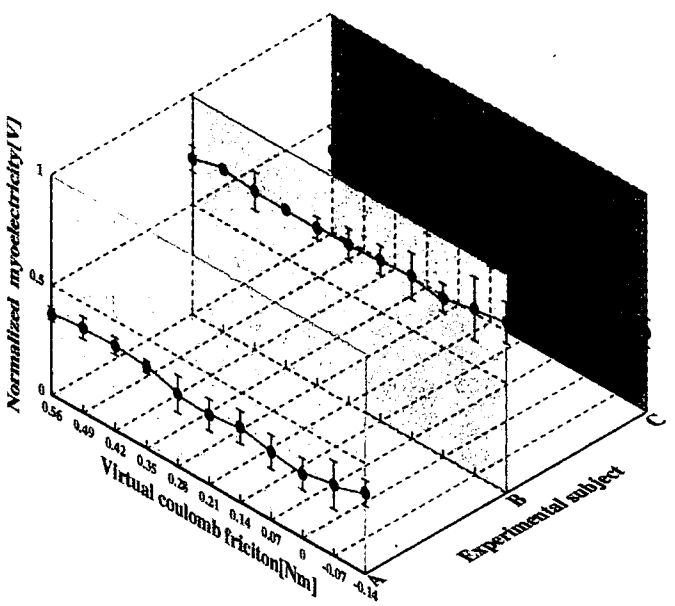

(b)

Figure 8. Experimental results for myoelectricity at the extensor muscle.

moment of the exoskeleton was large against the adjusted virtual viscous friction and the operators corresponded sensitively to the change of virtual viscous friction by increasing the impedance of muscles.

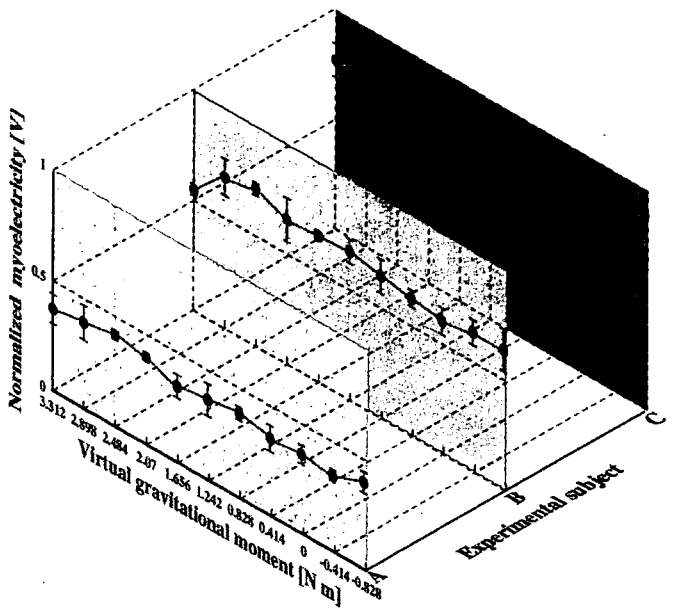

(a)

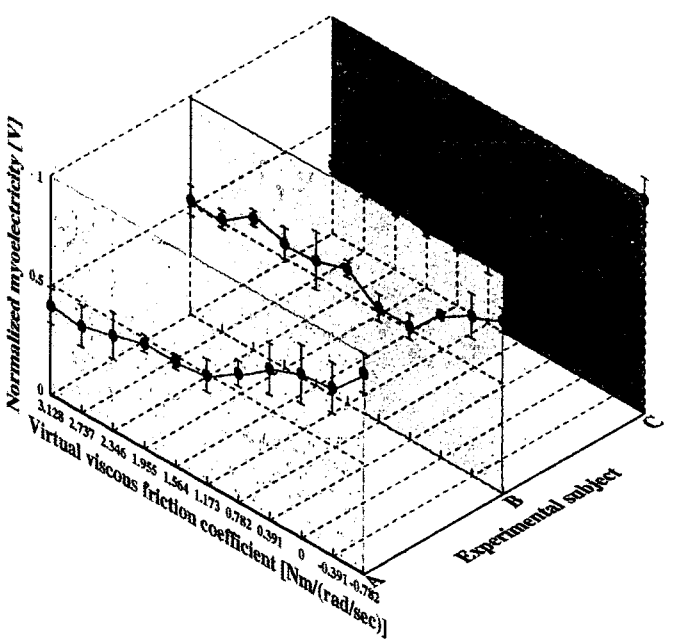

(b)

Figure 8. (Continued).

4.2. Experiments for adjustment of virtual impedance based on results of the basic experiments

Next, experiments for adjustment of the virtual inertia moment, viscous friction, gravitational moment and Coulomb friction were performed. Based on the results of the former experiments, the virtual inertia moment and the virtual Coulomb friction were set to zero. The virtual gravitational moment also needed to be adjusted properly to minimize the operator's physical stress, and its value was retained since the musculoskeletal moment and myoelectricity indicated the minimum values at the original gravitational moment of the exoskeleton. The virtual viscous friction was adjusted such as in the basic experiments and the experimental results were examined, again focused on the relationship between the change of the virtual viscous friction and the operators' physical stress. The experimental results were obtained from 220 trials for each operator.

Figure 9a–c shows the experimental data of the musculoskeletal moment, the operator's feelings and the myoelectricity at the flexor and extensor for operators A–C, respectively. The experimental results in panel (d) of Figs 6–8 are plotted as a graph of musculoskeletal moment and myoelectricity at the flexor and extensor with a shaded line, and vertical lines indicate the lowest points of the musculoskeletal moment with which the physical stress was mainly evaluated.

As an overall trend, the amounts of myoelectricity at the extensor and musculoskeletal moment decreased, and the myoelectricity at the flexor was reduced partially compared to the results in panel (d) of Figs 6–8. Hence, it is likely that the physical stresses by Coulomb friction and by inertia moment involving the decrease of the virtual viscous friction were reduced. However, the myoelectricity and musculoskeletal moment still increased at the lower value of virtual viscous friction, and, thus, it is likely that the operators increased the impedance of muscles against the reduced virtual viscous friction regardless of the adjustment of the virtual inertia moment.

The operationality and stress level measured by the SD method became worse and lighter with the decrease of the virtual viscous friction. Focusing attention on the musculoskeletal moment, the data from operators A–C had the common feature that amounts were lowest, and the marks of operationality and the stress level were in the range -1 to 1, at 1.56 N m/(rad/s) of the viscous friction coefficient. Thus, the graphs of the musculoskeletal moment and the operators' feelings in Fig. 9 tell us that if the minimum musculoskeletal moment was prioritized in order to set the criteria for the effective unconstrained motion, the marks for both operationality and stress level indicated medium values, and the virtual viscous friction was to be adjusted based on 1.56 N m/(rad/s). However, if the minimum myoelectricity was prioritized instead of the musculoskeletal moment, the virtual viscous friction coefficient should be higher than 1.56 N m/(rad/s), and the operationality and stress level measured by the SD method became better and heavier, respectively. If the condition of the ideal virtual viscous friction to minimize the physical stress of

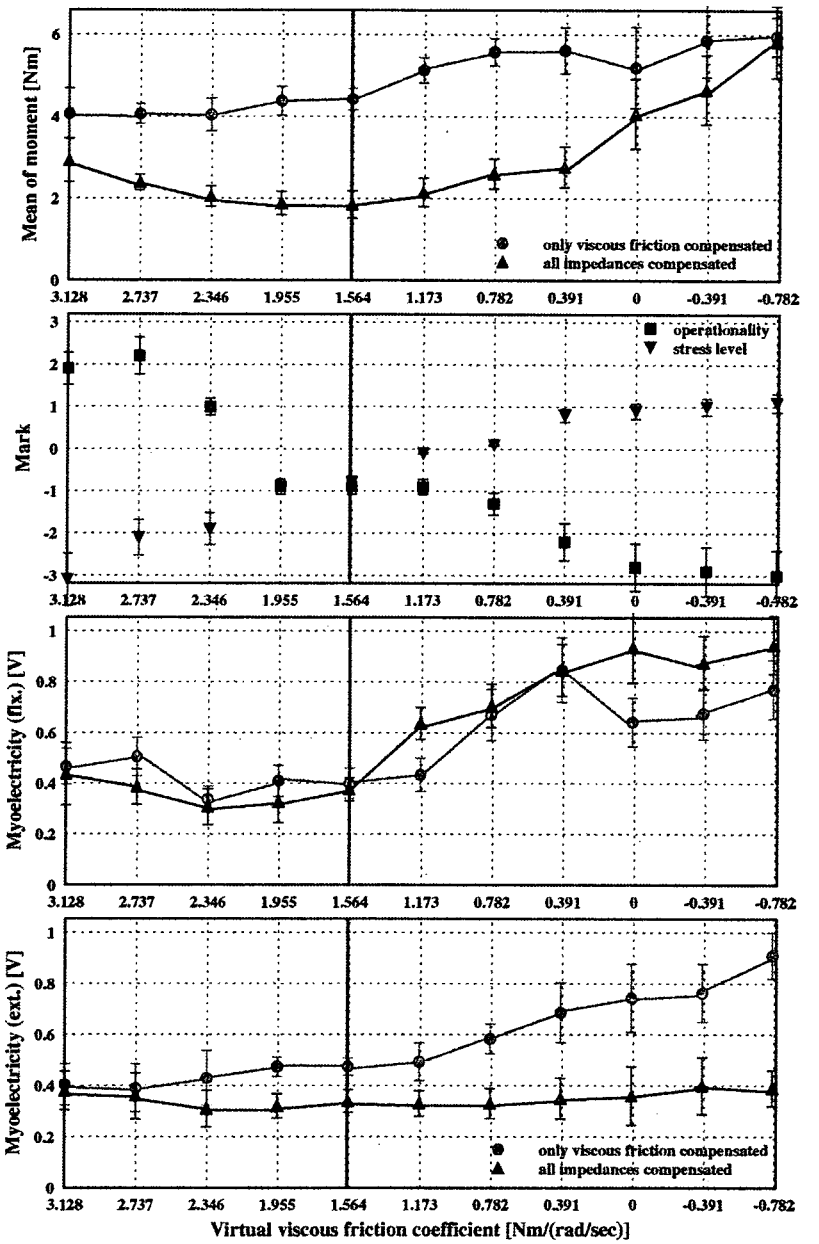

(a)

Figure 9. Experimental results for adjusting the virtual impedance based on the results of the basic experiments.

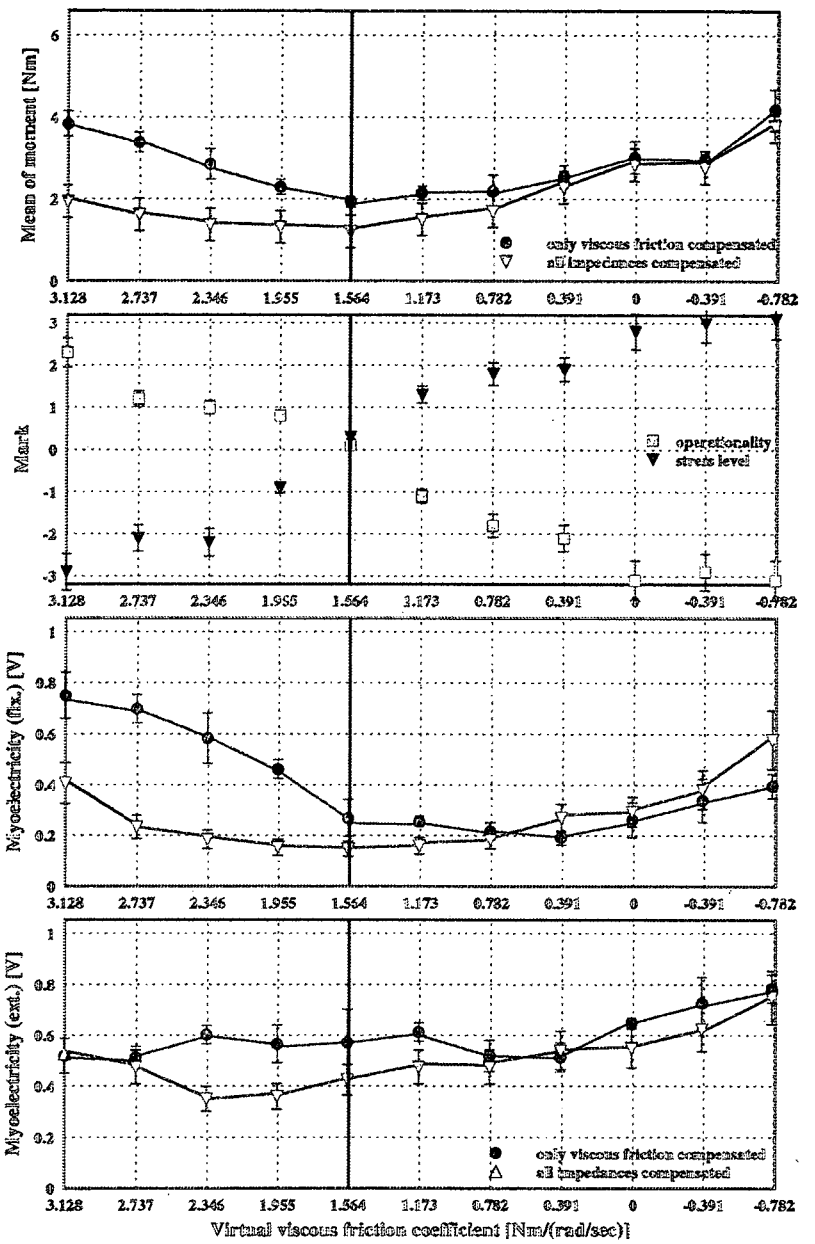

(b)

Figure 9. (Continued).

operators is to minimize the musculoskeletal moment and the muscle's activation as much as possible, the virtual viscous friction should be adjusted to a value a little higher than 1.56 N m/(rad/s).

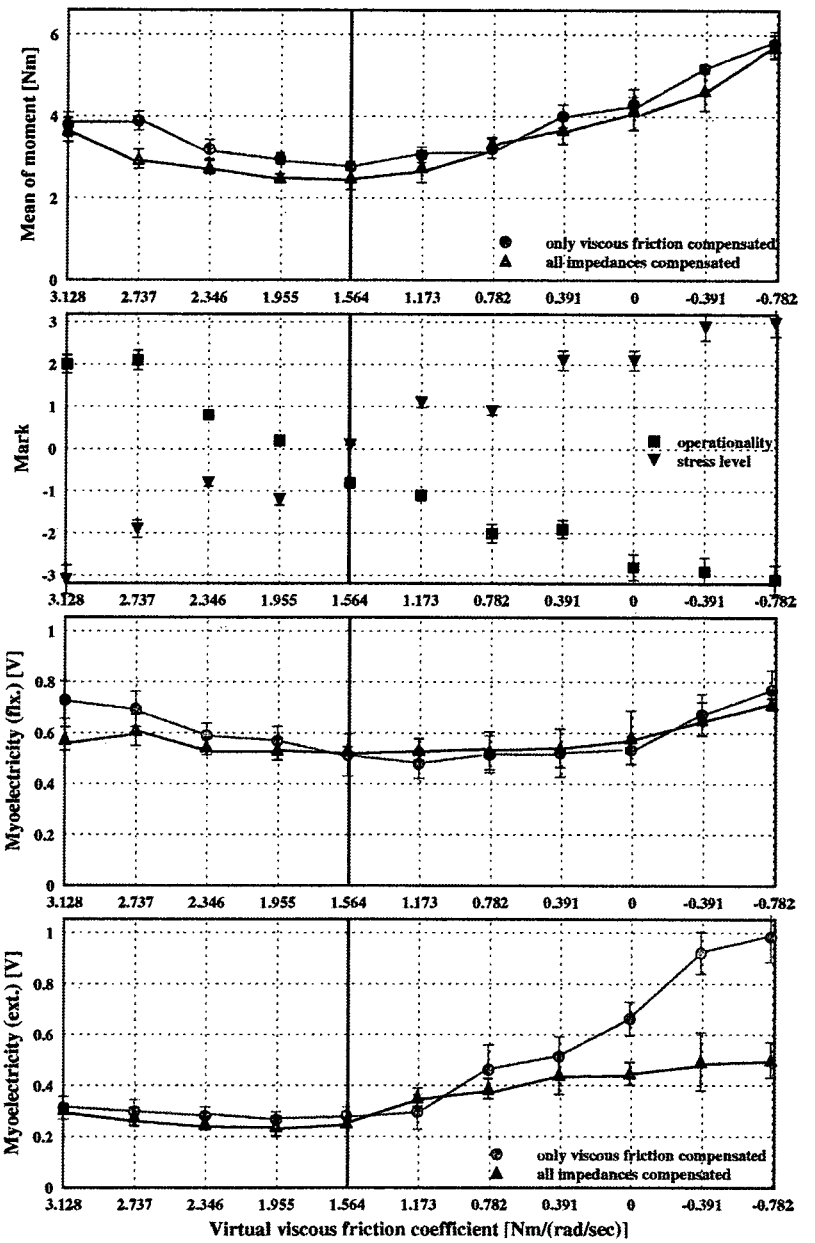

(c)

Figure 9. (Continued).

Therefore, based on the experimental results the criteria of the impedance adjustment for an exoskeletal robot assisting the unconstrained motion of the leg can be summarized as follows:

(i) Set the virtual inertia moment and the virtual Coulomb friction to zero, respectively.

(ii) The virtual gravitational moment should be retained.

(iii) The virtual viscous friction should be adjusted to be a value a little higher than the value of the virtual viscous friction coefficient in order to minimize the musculoskeletal moment. In the case of HAL-3, the virtual viscous friction coefficient was adjusted based on a value a little higher than 1.56 N m/(rad/s).

5. DISCUSSION

In Fig. 9a–c, the myoelectricity, which represents the muscle activation, was a little higher than its minimum value at the virtual viscous friction which made the amount of musculoskeletal moment lowest. Thus, it is likely that human operators increased the impedance around the joint by antagonist muscle action to realize effective unconstrained motion of the leg.

The musculoskeletal moment of operator A in Fig. 6d became the lowest at the higher value of the virtual viscous friction and it is likely that operator A corresponded sensitively to the change of virtual viscous friction compared to operators B and C. The stress level of operator A in Fig. 9a became lower than that of operators B and C at the minimum value of the musculoskeletal moment. Differences in feelings to the same experimental motion or proficiency for experiments was considered as the main cause of the results.

The operationality was not improved with the decrease of virtual viscous friction in the experimental result shown in Fig. 9 and it is considered that the viscous friction around HAL-3's actuators did not have any detrimental influence on the operationality of the operator. If the myoelectricity that represents muscle activation is prioritized in the evaluation of physical stress, the operationality has more influence on the human's feeling than the stress level in unconstrained motion.

The basic experiments for adjustment of the virtual inertia moment showed its influence on the operator's motion was comparatively small, although it was anticipated that the inertia moment of exoskeleton affected the musculoskeletal moment and muscle's activation greatly. The reason for this is that the inertia value was small compared that of a human [7] and the motions in the experiments were not rapid enough to be influenced by inertia change. However, it is expected that the influence of inertia moment will become larger when the change of angular velocity is very large.

6. CONCLUSIONS

We examined and evaluated the relationships between the virtual impedance values and the physical stress of operators through experiments for unconstrained motions of the lower leg, and could establish the criteria for adjusting the virtual impedance

of the exoskeletal robot for the lower limb in order to minimize the operator's physical stress in unconstrained motion. It is likely that effective assist of the unconstrained lower limb, such as a swung leg in walking, can be realized by applying the established criteria in this paper to an exoskeletal robot for the lower limb.

REFERENCES

1. J. Okamura, H. Tanaka and Y. Sankai, EMG-based prototype powered assistive system for walking aid, in: *Proc. Asian Symp. on Industrial Automation and Robotics (ASIAR '99)*, Bangkok, pp. 229–234 (1999).
2. T. Nakai, S. Lee, H. Kawamoto and Y. Sankai, Development of power assistive leg for walking aid using myoelectricity and linux, in: *Proc. Asian Symp. on Industrial Automation and Robotics*, Bangkok, pp. 1295–1310 (2001).
3. S. Lee and Y. Sankai, Power assist control for walking aid with HAL-3 based on EMG and impedance adjustment around knee joint, in: *Proc. IEEE/RSJ Int. Conf. on Intelligent Robots and Systems*, Lausanne, pp. 1499–1504 (2002).
4. H. Dankowicz, J. Adolfsson and A. B. Nordmark, Repetitive gait of passive bipedal mechanism in a three-dimensional environment, *J. Biomechan. Eng.* **123**, 40–46 (2001).
5. T. Tsuji, Y. Tanaka and M. Kaneko, Tracking control properties of human-robot systems, in: *Proc. 1st Int. Conf. on Information Technology in Mechatronics*, Istanbul, pp. 77–83 (2001).
6. Y. Yamada, H. Konosu, T. Morizono and Y. Umetani, Proposal of skill-assist: a system of assisting human workers by reflecting their skills in positioning tasks, in: *Proc. IEEE Int. Conf. on Systems, Man and Cybernetics*, Tokyo, pp. (IV)11–(IV)16 (1999).
7. S. Lee and Y. Sankai, Natural frequency-based power assist control for lower body with HAL-3, in: *Proc. IEEE Int. Conf. on Systems, Man, and Cybernetics*, Washington, DC, pp. 1642–1647 (2003).
8. E. Park and S. G. Meeek, Fatigue compensation of the electromyographic signal for prosthetic control and force estimation, *IEEE Trans. Biomed. Eng.* **40**, 1019–1023 (1993).
9. M. S. Ben-Lamine, S. Shibata, K. Tanaka and A. Shimizu, Impedance characteristics of robots considering human feelings, *JSME Int. J. (Ser. C)* **40**, 309–315 (1997).
10. H. I. Krebs, N. Hogan, M. L. Aisena and B. T. Volpe, Robot-aided neurorehabilitaion, *IEEE Trans. Rehabilitation Eng.* **6**, 75–86 (1998).

ABOUT THE AUTHORS

Suwoong Lee received the BS degree in Electrical Engineering from Dong-A University, Korea in 1999, and the MS degree in Intelligent Interaction Technologies from the University of Tsukuba, Japan in 2002. He has been pursuing the PhD degree in the Doctoral Program in Intelligent Interaction Technologies, University of Tsukuba since 2002. His research interests include biomechanics, biorobotics and the human–machine interface including assistive exoskeletal robots and haptic devices. He is a member of the Robotics Society of Japan, and the Japan Society of Mechanical Engineers.

Yoshiyuki Sankai received the PhD degree in engineering from the University of Tsukuba, Japan in 1987. He was a JSPS research fellow, Assistant Professor, Associate Professor and Professor of Institute of Systems and Engineering in the University of Tsukuba, and a Visiting Professor of Baylor College of Medicine in USA. Currently, he is a professor and director of the prioritized research area 'New Robotics Frontier: Cybernics', Graduate School of System and Information Engineering in University of Tsukuba, Japan. His research interests include Robot Suit HAL (Hybrid Assistive Limb), the next generation artificial heart, humanoid Control, Bio-Medical Science, Network Medicine as related fields of Cybernics. He received a Grant of the Japanese Society for Artificial Organs (JSAO), Awards from American Society for Artificial Organs, International Society for Artificial Organs, International Society for Rotary Blood Pump with his students and so on. He was/is a president of Japan Society of Embolus Detection and Treatment, a chair of *International Journal of the Robotics Society of Japan*, a member of Awards Committee in the Robotics Society of Japan and Japan Society of Mechanical Engineers, an executive editor of Vascular Lab., an executive board member of Robotics Society of Japan, a founder and a chairman of CYBERDYNE Inc.

Advanced Robotics, Vol. 19, No. 9, pp. 977–993 (2005)

Also available online - www.vsppub.com

Full paper

Three-dimensional link dynamics simulator based on *N*-single-particle movement

HIDEKI TODA * and YOSHIYUKI SANKAI

Doctoral Program of Systems and Information Engineering, Sankai Laboratory, University of Tsukuba, Tsukuba, Ibaraki, 305-0006, Japan

Received 31 August 2004; accepted 14 October 2004

Abstract—The purpose of this paper is to suggest a new three-dimensional multi-link system dynamics simulator. A 'Jacobian' matrix was generally used for calculating the dynamics of the multi-link system in previously proposed methods; however, this method has many difficulties related to the computational cost and precision of the calculations. For example, there are the problems of the singularity and the accumulation of calculation errors when it follows from the root to the end of the link, and the problems of treating external force effects in the angular space dynamics. In this study, we consider a multi-link system as a multi-particle movement system and each of the particles are connected by a kind of spring damper model as an imitation of a link. Using this mechanism, the Jacobian matrix is not required in the dynamics simulation and the complexity of the link dynamics simulation is dramatically decreased by way of introducing a rotational plane concept. We confirm the effectiveness of the simulator through some dynamics simulations such as walking.

Keywords: Three-dimensional multi-link simulator; robot control; link dynamics.

1. INTRODUCTION

Many multi-joint type robot systems have been recently proposed (WABIAN [1], HRP [2], ASHIMO [3], KHR-1 [4]) and used with the aim of imitating human movement [5]. The rationale for imitating human movement is to acquire a new movement which was impossible in previous studies and to search for a generating or learning mechanism of the movement which is closer to that of a human being. For realizing human movement, however, it is necessary to introduce expensive real robot systems and to prepare the environment of the system at the same time. In addition, we must include an algorithm to realize a task into the control system and confirm the effectiveness step by step. In this case, physical problems with the control system and performance deterioration of the motors or actuators can

*To whom correspondence should be addressed. E-mail: toda@golem.kz.tsukuba.ac.jp

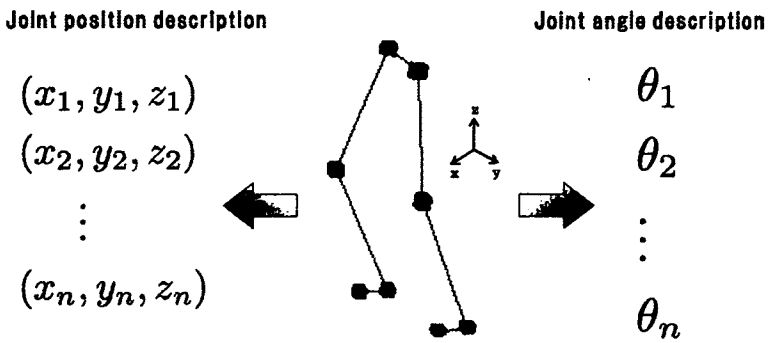

Figure 1. Joint position and angle description.

cause serious difficulties. When the movement does not go well, it is difficult to analyze it and understand if the reason lies in the control algorithm or the physical structure (kinematics) of the robot. If the purpose of using a real-world robot depends on ascertaining the role of the control algorithm and the effect through the experiments, the practical working difficulties will be equivalent to the cost of manufacturing an atomic bomb and ascertaining the explosive power. In addition, destructive influences such as a turnover or shock become very important factors and environmental effects such as the influence of the ground conditions (sandy or muddy) also become important when we consider the safety of the robot system.

Generally, in order to reduce experimental cost, a virtual world computer simulation (e.g. Open-HRP [6, 7], Human Figure [8]) or another mathematical calculation method [9, 10] is used. However, it produces some difficulties because precise modeling of the external environment and robot system itself is difficult. The major reasons depend on the fundamental principle of conversion equivalence between the work space coordination $\vec{x}$ and the angle state space $\vec{q}$, and this principle assures that we can change the work space coordinate into the angle state space coordinate, which is convenient for the calculation. However, this conversion has a singularity — in the case that there is no inverse matrix. In addition, there are problems of introducing external effects into the angular space dynamics and an accumulation of calculation errors when it follows from the root to the end of the link. In particular, influences of external forces or effects to be added in the link system often appear in the form of 'condition of the ground', 'shock from the external environment' or 'link vibration and distortion', and these influences are directly connected to the stability of the system. Each time these external factors increase, the influences must be analyzed and added into the link dynamics simulator in order to understand the dynamics phenomenon in the angular state space. For example, in the case of introducing unstable soft ground into the simulator, we must know the influence of the collision effect when a link touches ground and the effect of the ground motion itself. These factors are analyzed and added mathematically in the angular state space. In short, the dynamics phenomenon on the work space coordinate is difficult to convert into the angle state space. In almost all of the cases, these analysis and

conversion processes are very complex, and the precision of the simulation of the dynamics has fallen through the process of simplification. Each time we want to add environmental factors into the simulator, we must repeat these processes and reduce the degree of freedom of the simulator against the environments. These processes cause a heavy calculation load and the precision of the calculation is thus reduced. In this study, we propose a new multi-link dynamics simulator system which does not need to use the 'Jacobian' conversion process from work space to angle space or from angle space to work space in the link dynamics calculation. Our proposed method considers that the multi-link system is equivalent to a multi-particle system in which each of the particles is restricted by other particles. In other words, the system in which each of the particles is connected with a spring–damper model is considered as an approximation of the link movement in our method. Using this approximation, the amount of calculation is reduced dramatically and it is easy to introduce external dynamic factors of the environment in the proposed method.

2. DYNAMIC LINK MODEL DESCRIPTION

The proposed multi-link system description method does not utilize the angular expression method of the rigid body system which is used to describe the link dynamics in the previously proposed method. It does not use the joint angle state space, except when necessary. The position relation of the joint on the work space is used in order to describe the joint angle. An expression of the joint angle becomes possible if there are at least three points on the work space as shown in Fig. 2a. We consider that each of the points is connected by some kind of restriction condition. Although any kind of restriction condition may be used, we selected the spring–damper model as the restriction condition due to reasons of simplicity and stability (Fig. 2b).

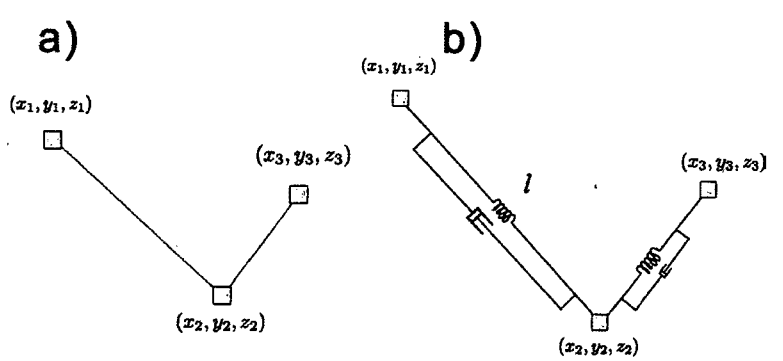

Figure 2. Link position description as a spring–damper model.

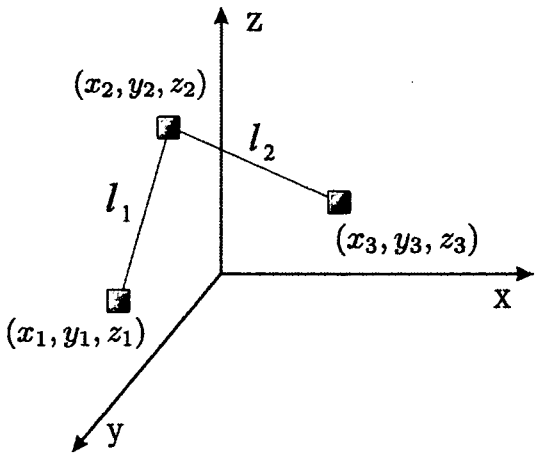

Figure 3. The joint representation constructed from three particle points.

Each particle receives some force from the other particles under the conditions of presuming a spring–damper model and this system cannot move in any free direction.

As shown in Fig. 3, one joint is constructed when one particle is restricted at a distance l from the other two particles. This restriction condition is very important for treating rigid body dynamics as 'the system has the size'. For introducing the motion equation of the multi-link system under the restriction condition of the spring–damper, we define the Lagrangian of the system with only three particle points in the three-dimensional space:

$$\begin{aligned} L &= T - G \\ &= \frac{1}{2}m_1\dot{\vec{x}}_1^2 + \frac{1}{2}m_2\dot{\vec{x}}_2^2 + \frac{1}{2}m_3\dot{\vec{x}}_3^2 - \frac{1}{2}K\Delta l_1^2 - \frac{1}{2}K\Delta l_2^2 \end{aligned} \tag{1}$$

where $\vec{x}_1 = (x_1, y_1, z_1), \vec{x}_2 = (x_2, y_2, z_2), \vec{x}_3 = (x_3, y_3, z_3)$, L is the Lagrangian, T is the kinetic energy, G is the potential energy of the spring, K is the friction coefficient of the damper 1 and damper 2, and m_1, m_2 and m_3 are equal to mass of each particle. We define Δl_1 and Δl_2 as:

$$\begin{aligned} \Delta l_1 &= l_1 - |\vec{x}_1 - \vec{x}_2| \\ \Delta l_2 &= l_2 - |\vec{x}_3 - \vec{x}_2| \end{aligned} \tag{2}$$

Using the method of the Euler–Lagrange equation:

$$\frac{\partial L}{\partial \dot{\vec{x}}_1} = m_1\dot{\vec{x}}_1 \tag{3}$$

$$\frac{\partial L}{\partial \vec{x}_1} = 2K(\vec{x}_1 - \vec{x}_2) \cdot \left[1 - \frac{l_1}{|\vec{x}_1 - \vec{x}_2|}\right] \tag{4}$$

The motion equation $\vec{x}_1$ of the particle 1 is:

$$\frac{d}{dt}\frac{\partial L}{\partial \dot{\vec{x}}_1} - \frac{\partial L}{\partial \vec{x}_1} = 0 \tag{5}$$

That is:

$$m_1 \ddot{\vec{x}}_1 = -2K(\vec{x}_1 - \vec{x}_2) \cdot \left[1 - \frac{l_1}{|\vec{x}_1 - \vec{x}_2|}\right] \tag{6}$$

By defining $l_{12} = |\vec{x}_1 - \vec{x}_2|$, we obtain:

$$m_1 \ddot{\vec{x}}_1 = -2K(\vec{x}_1 - \vec{x}_2)\left[1 - \frac{l_1}{l_{12}}\right] \tag{7}$$

The singular point is created when the position $\vec{x}_1$ equals $\vec{x}_2$. However, because the two particle positions are thought to be connected with a spring, we can consider that the singular point is not created. It only occurs under a large external force, with the spring completely contracted.

Other coordinate motion equations are represented as:

$$m_1 \ddot{\vec{x}}_1 = -2K(\vec{x}_1 - \vec{x}_2)\left[1 - \frac{l_1}{l_{12}}\right] \tag{8}$$

More importantly, the effect of the number of restriction conditions directly appears in the Lagrangian function as simply increasing the number of terms and it appears in the motion equation as simply increasing the number of terms. For example, the motion equation of particle 2 is represented as:

$$\begin{aligned} m_2 \ddot{\vec{x}}_2 = &+2K(\vec{x}_1 - \vec{x}_2)\left[1 - \frac{l_1}{l_{12}}\right] \\ &-2K(\vec{x}_3 - \vec{x}_2)\left[1 - \frac{l_2}{l_{23}}\right] \end{aligned} \tag{9}$$

where l_{23} is the distance between particles 2 and 3. The motion equation of particle 3 is:

$$m_3 \ddot{\vec{x}}_3 = -2K(\vec{x}_3 - \vec{x}_2)\left[1 - \frac{l_2}{l_{23}}\right] \tag{10}$$

We can understand that (9) has two spring–damper restriction conditions from particles 1 and 3, and (10) has one restriction condition from particle 2. This means that the number of restriction conditions never increases the complexity of the motion equation and is directly proportional to the number of restriction conditions.

When we consider the motion dynamics by using the angular state space, we need to resolve the angular acceleration level dynamics of the system. If the dynamics include the free work space movement, the description will be complicated by the center of mass movement and the rotation or relative movement. However, our proposed method does not need to consider those coordinate conversions. For

example, a fixed position can be described very simply by way of $\dot{\vec{x}}_i = 0$ and $\ddot{\vec{x}}_i = 0$, but these restriction conditions are difficult to treat in the angular state space description. In addition, our approach does not depend on whether a link is closed or open at all, e.g., the open link in Fig. 3 can converted into a closed link by connecting the joint coordinates 1 and 3 by a spring–damper; motion equations (8) and (10) just have two terms, respectively, such as in (9) and the unstable computational structure does not occur:

Our proposed method is very simple, but there are some difficulties:

(i) Each particle position has a small vibration.

(ii) There is no rotation restriction of the joint.

(iii) It cannot represent the torque or the friction effects in the system.

Below, we describe each of these points.

3. THE DEFINITION OF THE ROTATION PLANE

Since each particle is connected by the spring system, the first problem is clear. However the vibration effects can be inhibited by using other factors such as compliance or friction effects of the spring system. If vibration does occur, the conservation of mechanical energy of the link system is not maintained. In real world motion dynamics, energy dissipation occurs in the aluminum or iron link, and we can explain that the dissipation is converted to internal grid motion and disappears as thermal energy. In addition, we can introduce a very large external impulse by using the solid-state properties such as 'thermal' effects or expansion or contraction.

The next problem is rotation restriction. The joint movement equations (8)–(10) represent 'spherical joint' dynamics, such as in a hip joint, but a general serial link has only one motor and is restricted to a single rotation axis. Figure 4 represents three particles and a surface which is spanned by the three points. We define this surface as the 'rotation plane'. The surface has a normal vector $\vec{n}$ and we construct the restriction that the three particles can move only in the rotation plane.

First, we calculate $\ddot{\vec{x}}_1$, $\ddot{\vec{x}}_2$ and $\ddot{\vec{x}}_3$ of the three particles. Next, we delete the acceleration factor parallel to the normal vector (Fig. 5). For example, by using the normal vector $\vec{n}$ and $|\vec{n}| = 1$, the acceleration factor parallel to $\vec{n}$ is represented as:

$$\vec{a}^n = (\vec{n} \cdot \vec{a}_1)\vec{n} \tag{11}$$

By deleting the parallel factor:

$$\vec{a}^{\text{new}} = \vec{a} - \vec{a}^n = \vec{a} - (\vec{n} \cdot \vec{a})\vec{n} \tag{12}$$

The acceleration term $\vec{a}^{\text{new}}$ is used instead of $\vec{a}$. We can define the rotation joint which has a single rotation axis by using this process.

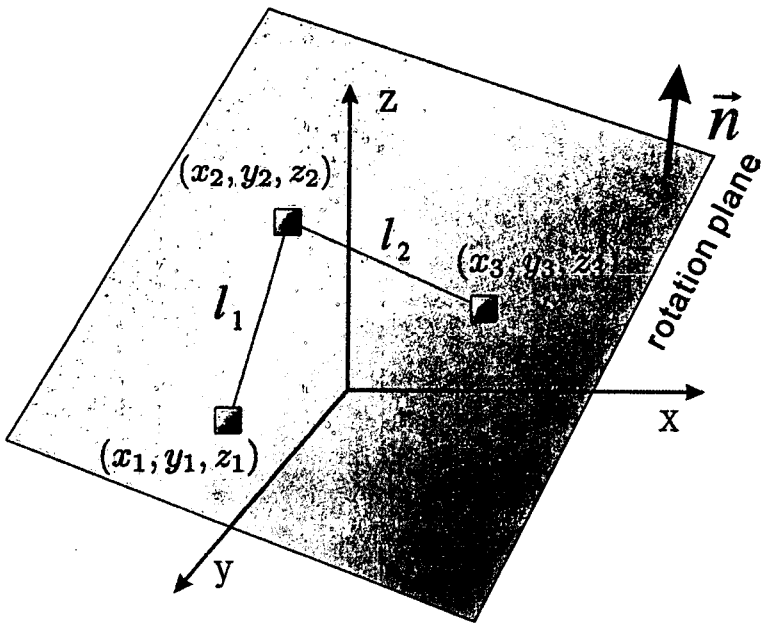

Figure 4. Rotation plane.

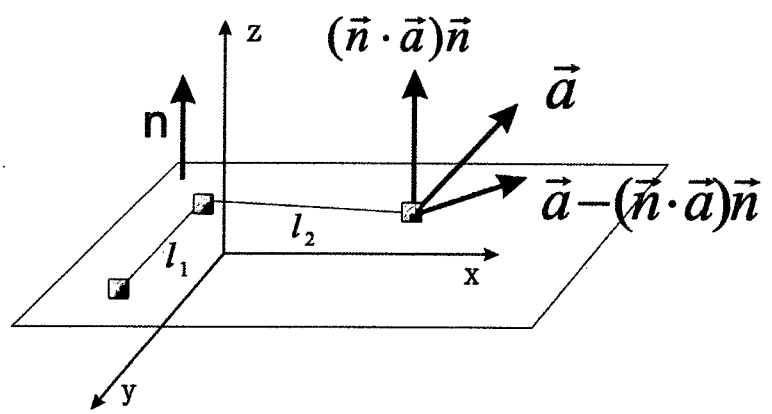

Figure 5. Acceleration decomposition.

3.1. Torque effect

For simplifying the torque effect descriptions of the joint movement, we consider the one-dimensional space movement of two particles (Fig. 6). There is no friction in the system, and the two particles are in touch with the spring and not connected to each other. If the spring becomes stretched, the two particles move separately. This shows that there is no center of mass movement and that only relative movement has occurred (Fig. 6c).

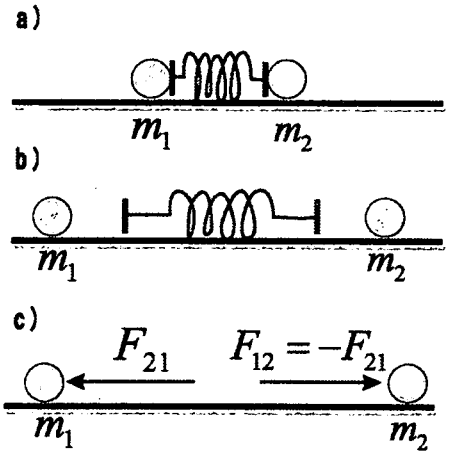

Figure 6. One-dimensional movement of two particles. (a) Initial state. (b) The presence of internal force. (c) $F_{12} = -F_{21}$.

The motion equation is:

$$m_1\ddot{x}_1 = F_{21} + F_1^{ex} \tag{13}$$

$$m_2\ddot{x}_2 = F_{12} + F_2^{ex} \tag{14}$$

where F_1^{ex} is the external force to particle 1 and F_{21} is the internal force, and there is a simple relationship $F_{21} = -F_{12}$. That is the law of action and reaction. We consider the case of $F_1^{ex} = 0$ and $F_2^{ex} = 0$, and the relative movement equation $x = x_1 - x_2$ is:

$$\frac{m_1 m_2}{m_1 + m_2}\ddot{x} = F_{12} \tag{15}$$

where μ means the conversion mass $\mu = \frac{m_1 m_2}{m_1 + m_2}$:

$$\mu\ddot{x} = F_{12} \tag{16}$$

When we apply it to the rotation movement, the key point is that the internal force F_{12} is equivalent to the torque effect and it is the force which tries to open a joint angle as an internal force. We can consider this situation in the rotation movement, where the motion equation is:

$$I_1\ddot{\theta}_1 = \tau_{21} = \tau \tag{17}$$

$$I_2\ddot{\theta}_2 = \tau_{12} = -\tau \tag{18}$$

where I_1 and I_2 are of the momentum values and θ_1 and θ_2 are the rotation angles of mass 1 and 2. The important point is that the torque τ can be treated as an internal force and we can separate it in to the movement of two particles (Fig. 7).

The force f_1 which is generated by the torque τ in a distance l_1 (Fig. 8):

$$f_1 = \frac{\tau}{l_1} \tag{19}$$